

Electronic supplementary information for:  
**Shock-induced collapse of surface nanobubbles**

Duncan Dockar,<sup>\*,a</sup> Livio Gibelli,<sup>a</sup> and Matthew K. Borg<sup>a</sup>

DOI link to dataset: <https://doi.org/10.7488/ds/3096>

## Contents

<b>1 Measurement techniques</b>	<b>1</b>
1.1 Shock-wave	1
1.2 Velocity	1
1.2.1 Mean velocity	1
1.2.2 Jet profile	2
1.3 Pressure	2
<b>2 Movie file captions</b>	<b>4</b>

### 1 Measurement techniques

In this section, we detail some of the measurement techniques employed in our article, with additional discussions on associated statistical errors in example cases.

#### 1.1 Shock-wave

Pressure was measured in region  $50 < z < 55$  nm (where  $z = 0$  nm is defined at the substrate surface), during shock-wave propagation in the “no-bubble” case, and is shown as a function of time in Figure S1. The first peak of this curve corresponds to the measured shock-

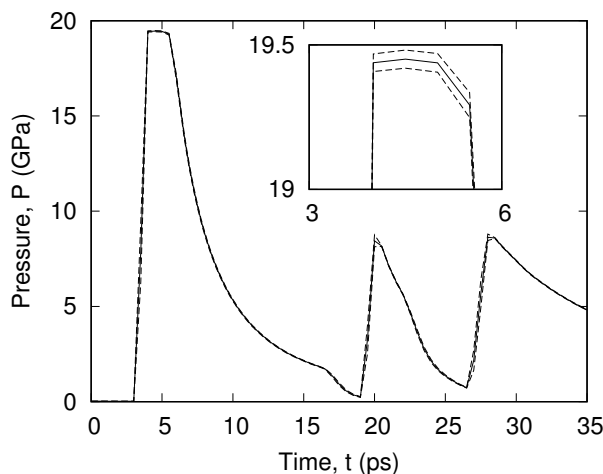


**Figure S1** Variation in shock-wave pressure with time for the no-bubble case, measured in region  $50 < z < 55$  nm (where  $z = 0$  nm is defined at the substrate surface). The solid black line shows the measured pressure, while the dashed lines show the uncertainty, to three standard errors. The inset shows the peak pressure measurement in more detail.

wave pressure,  $19.45(\pm 0.03)$  GPa, as described in the main article, while the next two peaks correspond to the shock-wave reflections off the substrate and top piston, respectively.

#### 1.2 Velocity

##### 1.2.1 Mean velocity

We compute the (mass) weighted mean velocity in each cylindrical-shell bin:<sup>1</sup>

$$\vec{u} = \frac{\sum_i' m_i \dot{\vec{r}}_i}{\sum_i' m_i}, \quad (1)$$

\*E-mail: d.dockar@ed.ac.uk

<sup>a</sup> School of Engineering, Institute of Multiscale Thermofluids, The University of Edinburgh, Edinburgh EH9 3FB, UK

where  $\vec{u}$  is the mean velocity vector in a given bin, and  $m_i$  and  $\vec{r}_i$  are the mass and velocity vector of atom  $i$ , respectively. The prime symbol in both summations indicate that only atoms within the bin are to be summed.

As an example, in Figure S2(a), we plot the  $z$  and  $r$  component velocities of the 40nm spherical vapour nanobubble case, at  $t = 9.95$ ps, just before the jet impacts the substrate. We also compute the standard error, from the variance of atomic velocities in each

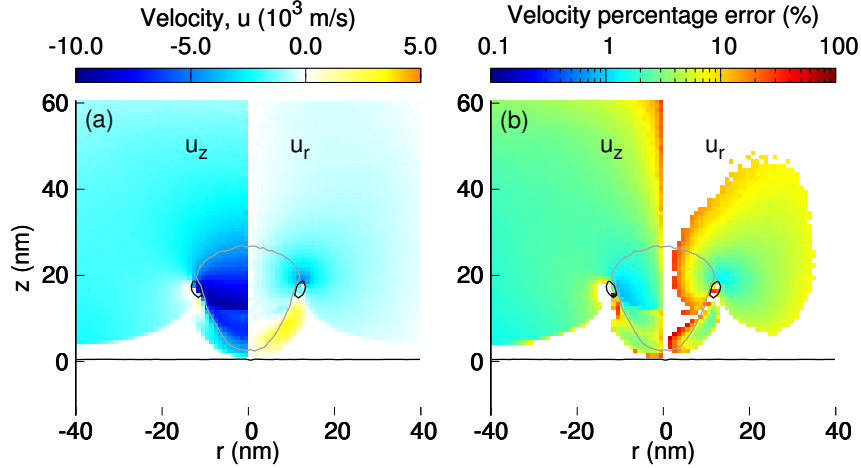


**Figure S2** Variation in: (a) velocity, and (b) percentage error in velocity, given to three standard errors, at  $t = 9.95$ ps, for the 40 nm diameter spherical vapour nanobubble collapse. The black lines show the bubble and substrate surfaces where possible, and the dark-grey line shows the jet profile. The figures are shown in cylindrical coordinates, with the  $z$  axis defined through the centreline of impact, and  $r$  is the radial component from the centreline. The left and right-hand sides of each plot shows the  $u_z$  and  $u_r$  velocity components, respectively. Errors in (b) are omitted for velocity component magnitudes:  $u_r, u_z < 500$ m/s.

bin, which is shown for the  $z$  and  $r$  velocity components in Figure S2(b). We do not show the errors for velocity component magnitudes  $u_r, u_z < 500$ m/s, as these are outside of the range of interest for our jet and shock-wave velocity analyses.

The errors associated with the velocity measurements are expected to be inversely proportional to the square root of the number of particles in the bin (which is dependent on radial component  $r$ ), and also the Mach number ( $u/c_{0,l}$ , where  $c_{0,l} = 2300$ m/s is the speed of sound in the liquid), and we see in these regions of interest, the errors are suitably low.<sup>2</sup>

### 1.2.2 Jet profile

At each time-step, we defined a jet profile in our simulations (see Figures 4–6 in the main article), which we used to measure and compare jet velocities across the different bubble sizes and types, by analysing the jet’s momentum density:  $\rho u_j$ , which is the product of the density  $\rho$  and the  $z$  component velocity pointing towards the wall  $u_j$ . In our analysis, we define the jet profile as the 50% iso-momentum density contour, which is the interface defined by the mid-point value between the mean momentum density within the bulk part of the jet profile and the momentum density of the plane shock-wave ( $3.5715 \times 10^6$  kg m/s, as measured from the no-bubble case). Since the definition of this profile required averaging of the momentum density within the profile itself, we had to iteratively repeat these steps to obtain a converged solution for the final jet profile.

For example, we show the tracking of the jet profile at each iteration in Figures S3(a)–(e), for the 40nm spherical nanobubble, at  $t = 8.8$ ps. For the first iteration in Figure S3(a), we plot the 50% iso-momentum density contour, using the mean jet momentum from the previous time-step. We calculated the mean momentum density within this jet profile, as shown by the red highlighted bins, which were used to define the jet profile in the next iteration. This step was repeated, and the measured jet momentum and volume  $V_{jet}$  was found to converge after around five iterations, as shown in Figure S3(f). The final jet profile for this time-step is shown with the  $z$  and  $r$  component velocities in Figure S3(g).

Once the jet profile had been defined, we measured the weighted average velocity within this jet from:  $u_j = \sum_n^{N_{bin}} \rho_n u_{j,n} / \sum_k^{N_{bin}} \rho_k$ , where subscript  $n$  denotes the bin, out of a total  $N_{bin}$  bins within the jet region (similar to Equation (1)), and this jet velocity is shown in Figures 3(d)–(f) in the main article, as a function of normalised time.

### 1.3 Pressure

Local pressure variations were computed using the virial theorem:

$$P = \frac{1}{3} \left[ \sum_i' m_i |\dot{\vec{r}} - \vec{u}|^2 + \frac{1}{2} \sum_i' \sum_{k \neq i} \vec{F}_{ik} \cdot \vec{r}_{ik} \right] \frac{1}{V_{bin}}, \quad (2)$$

where  $P$  is the pressure in a given bin,  $\vec{F}_{ik}$  and  $\vec{r}_{ik}$  are the force and radial separation between atoms  $i$  and  $k$ , respectively. The prime symbols again indicate only atoms within the selected bin are to be summed. The first summation term in the square brackets in Equation (2) is often referred to as the *kinetic* contribution, which is closely related to the temperature, as given by:

$$T = \frac{1}{N_{DoF} k_B} \sum_i' m_i |\dot{\vec{r}} - \vec{u}|^2, \quad (3)$$

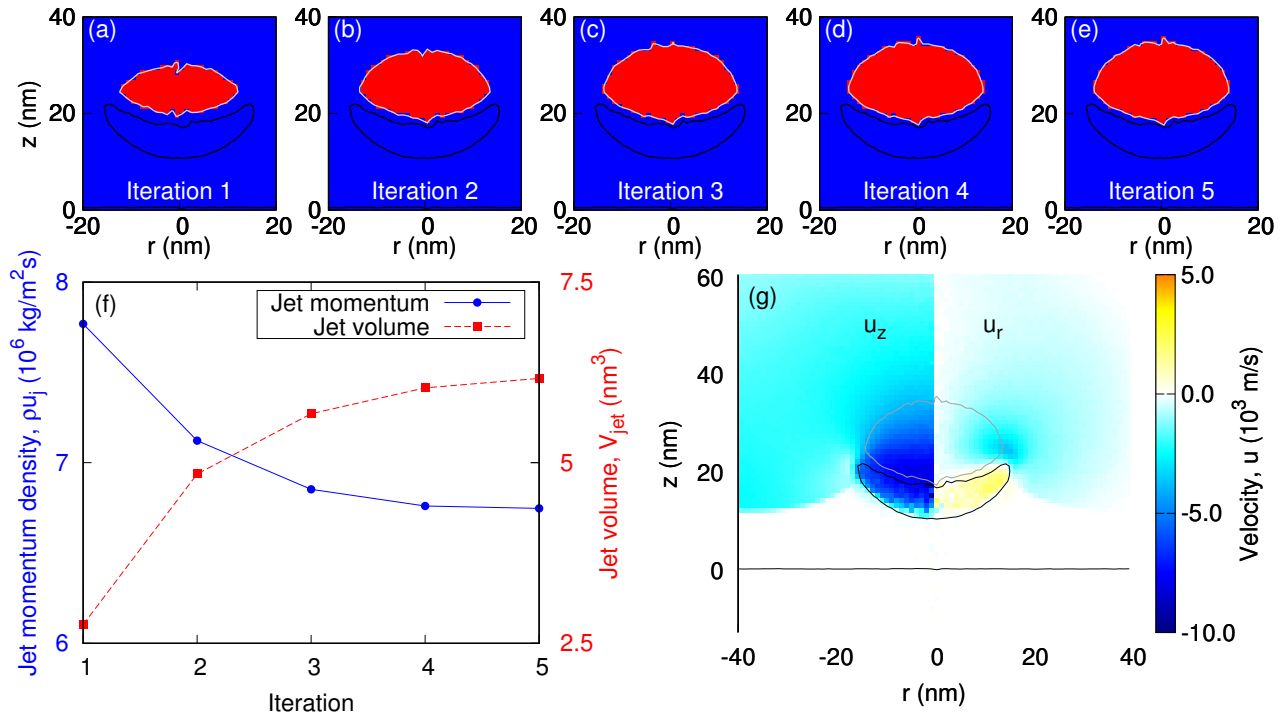


**Figure S3** (a)–(e) Iterations 1–5 of the 50% iso-momentum density jet profile determination, for the 40 nm diameter spherical nanobubble case, at  $t = 8.8$ ps; in each iteration, the black lines show the fixed bubble surface, the jet profile is shown as the solid grey line, while the bins within this jet profile are highlighted in red. All other bins are shown in blue. (f) Variation in jet momentum density  $\rho u_j$  and jet volume  $V_{jet}$  with iteration number. (g) Variation in velocity; the black lines show the bubble and substrate surfaces where possible, and the grey line shows the jet profile, obtained from the final iteration. (a)–(e) and (g) are shown in cylindrical coordinates, with the  $z$  axis defined through the centreline of impact, and  $r$  is the radial component from the centreline. The left and right-hand sides of (g) shows the  $u_z$  and  $u_r$  velocity components, respectively.

where  $N_{DOF}$  is the total number of degrees of freedom of all the atoms in the bin, and  $k_B$  is the Boltzmann constant. Both the kinetic contribution from Equation (2), and the temperature in Equation (3), subtract the mean local flow velocity  $\bar{u}$ , from the individual atomic velocities, using Equation (1), to operate only on the thermal kinetic energy.<sup>1,3</sup>

The second bracketed term in Equation (2) is the *potential* contribution, resulting from forces between pairs of atoms. While the first summation of this term only accounts for the atoms within the chosen bin, the second summation loops over all other atoms in the full domain. This approach is consistent with the virial theorem when one takes the bin volume as the volume of the full (periodic) domain, however, Hardy<sup>1</sup> discusses how the use of this particular formulation in Equation (2) could result in discrepancies from the momentum and energy conservation laws, due to incorrect weighting of forces from atoms acting outside of the bin. Hardy<sup>1</sup> also suggested that any such errors would be expected to be statistical (i.e. added noise), which we believe would be minimised from our high particle counts when employing cylindrically symmetric binning, and we will confirm this below. We also acknowledge that some concerns may be raised with the definition of pressure in Equation (2) when employed to non-equilibrium conditions, such as when there is a high-speed pressure wave passing through the system, as in our simulations.

To address these concerns, we have run several NVT simulations of bulk monatomic water (mW) model, in a periodic cube of size  $3.92 \times 3.92 \times 3.92 \text{ nm}^3$ , at various densities (by varying the number of particles from 1000–4028) and temperatures (between 300K–15000K, controlled by a Nosé–Hoover thermostat). Once each system had reached equilibrium, we measured the pressure using Equation (2), averaging over 0.5ns. The definition of pressure in this equilibrium system is not questionable, as highlighted by Hardy<sup>1</sup>, and serves as a useful benchmark for comparisons with the collapsing nanobubble results. Figure S4(a)–(c) shows the local variations in measured density, pressure, and temperature, respectively, in cylindrical coordinates, at  $t = 11.5$ ps for the 40nm spherical nanobubble collapse case, just after the jet impacts the substrate. We then compare the results of each bin element to the density-pressure-temperature values from our equilibrium NVT simulations, in Figures (S4)(d)–(i), at various temperature ranges. Error bars in the pressure are shown to three standard errors, computed by the variance of atomic stresses in each bin.

Despite the multiple shock-wave reflections and interference at jet impact, we see that the thermodynamic properties of the mW model in the nanobubble collapse simulations are still in good agreement with the equilibrium results. From this, we conclude that the pressure formulation in Equation (2) has been suitable for measuring the local pressure variations in our work.

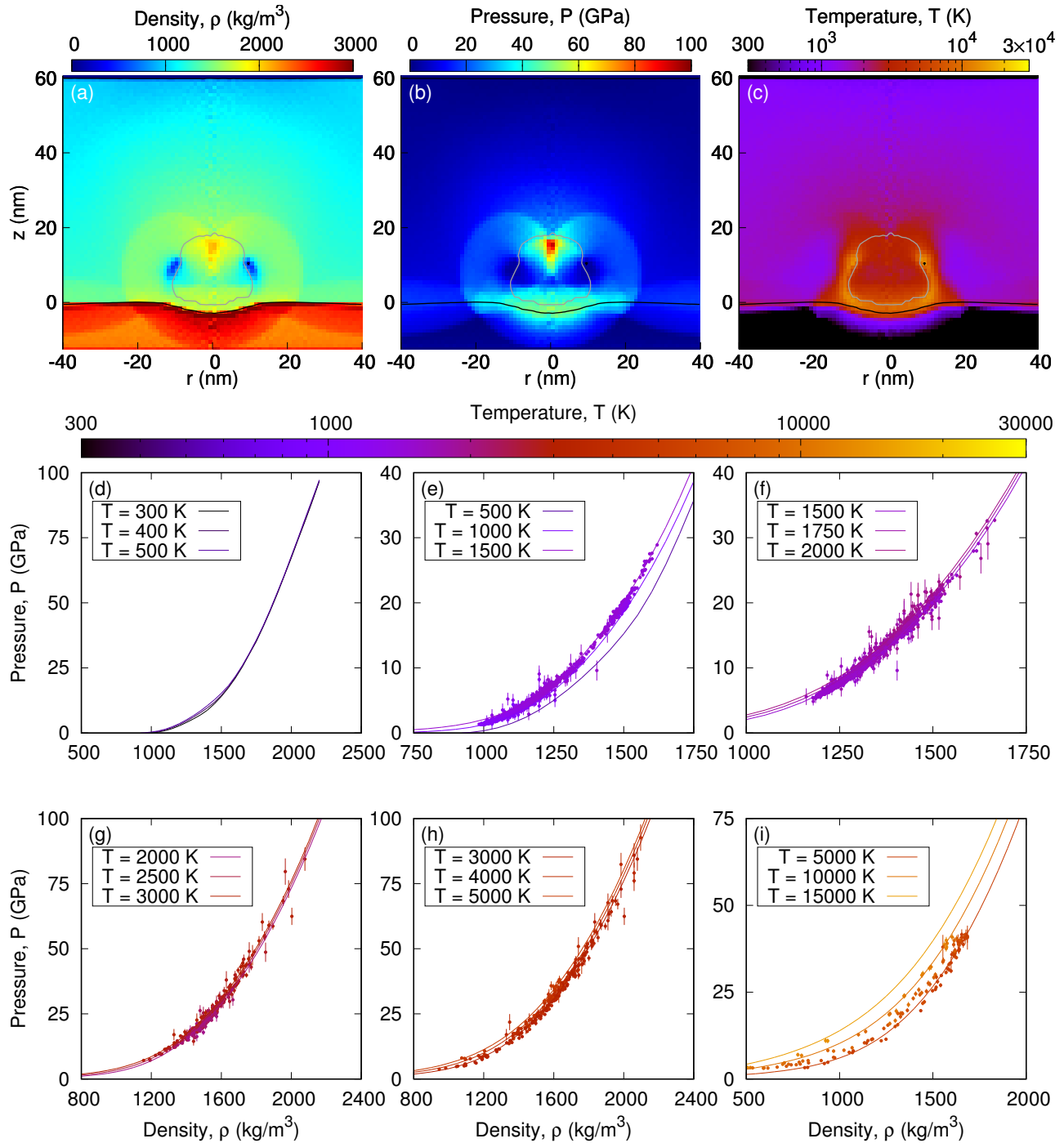


**Figure S4** Variations in: (a) density, (b) pressure, and (c) temperature, at  $t = 11.5\text{ps}$ , for the 40 nm diameter spherical vapour nanobubble collapse, in cylindrical coordinates, with the  $z$  axis defined through the centreline of impact, and  $r$  is the radial component from the centreline. The black lines show the bubble and substrate surfaces where possible, and the dark-grey line shows the jet profile. Variation in pressure with density, for temperature ranges: (d) 300–500K (e) 500–1500K, (f) 1500–2000K, (g) 2000–3000K, (h) 3000–5000K and (i) 5000–15000K. Each circle symbol represents one bin taken from (a)–(c), with colour denoting temperature as given by the legend, and error bars shown for pressure to three standard errors.

## 2 Movie file captions

**Movie 1** *40nm\_Spherical.mp4* 40nm diameter spherical nanobubble collapse

**Movie 2** *40nm\_HCA.mp4* 40nm diameter high contact angle (HCA) surface nanobubble collapse

**Movie 3** *40nm\_LCA.mp4* 40nm diameter low contact angle (LCA) surface nanobubble collapse

The following subfigure captions apply to each movie file:

- (a) Molecular Dynamics (MD) simulation rendering; the monatomic water (mW) molecules are shown in light-grey, monatomic nitrogen (mN) molecules in green, the hydrophobic (aSi<sub>o</sub>) and hydrophilic (aSi<sub>i</sub>) substrate atom types in yellow and dark-grey, respectively, and the piston (Ps) atoms in dark-blue. The renderings show a thin slice through the centre of the three-dimensional (3D) MD simulations. The mW molecules on the right-hand side of each image are not shown to improve the view of the bubble;
- (b) density  $\rho$ ;
- (c) velocity  $u$ , each plot is split in half at the centreline of the bubble impact: the left side shows the  $z$  component velocity, while the right side shows the  $r$  component velocity;
- (d) vorticity (azimuthal component)  $\eta_\phi$ ;
- (e) pressure  $P$  (side view);
- (f) pressure  $P$  (top view), measured in  $z = 1$  nm.

Subfigures (b)–(e) are shown in cylindrical coordinates, with the  $z$ -axis defined through the centreline of impact, and  $r$  is the radial component from the centreline; the black lines show the bubble and substrate surfaces, and the dark-grey line shows the jet profile. (f) is shown as a top-view, from the cylindrical binned data, rotated around the  $z$ -axis; the dashed white and solid black circles show the initial bubble and final pit diameters, respectively.

## References

- [1] R. J. Hardy, *J. Chem. Phys.*, 1982, **76**, 622–628.
- [2] N. G. Hadjiconstantinou, A. L. Garcia, M. Z. Bazant and G. He, *J. Comput. Phys.*, 2003, **187**, 274–297.
- [3] J. H. Irving and J. G. Kirkwood, *J. Chem. Phys.*, 1950, **18**, 817–829.